

## **Analysis of the Shell Structure under Extreme Load**

\*Joon-Ki Hong<sup>1)</sup> and Thomas Kang<sup>2)</sup>

<sup>1), 2)</sup> *Department of Architecture & Architectural Engineering,  
Seoul National University, Seoul, Korea*

<sup>2)</sup> [tkang@snu.ac.kr](mailto:tkang@snu.ac.kr)

### **ABSTRACT**

For containment structures, accidents caused by extreme environmental conditions should be considered even if it is highly improbable. Therefore all containment structures should observe the design code meticulously. As a role of preventing release of radiological materials, containment structures should resist beyond the design pressure. The main purpose of this study is to characterize the response of the reactor building with an analysis when a containment structure is under 0.7 MPa. The analysis is conducted using ETABS 2015. It is concluded that structural behavior of the containment structure can be analyzed using the tensile force and bending moment at various points, and that the critical point is located at 11 m in height of the modeled full-scale shell structure.

### **1. INTRODUCTION**

The three-mile island accident happened in the United States in 1979. In 1986, the Chernobyl disaster occurred. Recently, the explosion of a nuclear plant caused by the earthquake in Fukushima, Japan occurred in 2011. After these accidents, anxieties about structural safety of nuclear power plant (NPP) structures are stretched to the world. During the design of nuclear containment structures, nuclear structural engineers should consider various loading cases although it is highly improbable. For many kinds of accidents, severe accidents in the NPP structures are related to the loss of coolant accident (LOCA). In the event of a severe accident, radioactive materials are released, coinciding with increasing internal pressure level beyond the design pressure. Consequently, the NPP structure should perform a role as a radiation shield.

In general, NPP structures are typically comprised of main buildings, appurtenances, and foundation. The NPP structures are designated separately as safety-related or non-safety-related components. Reactor buildings and auxiliary buildings are classified as safety-related components constructed as concrete

---

<sup>1)</sup> Graduate Student

<sup>2)</sup> Associate Professor

structures. The reactor buildings consist of pressure boundary parts, such as cylindrical wall, hemispherical dome-shape roof and foundation slab, and internal structures which are not belonged to the pressure boundary parts. While the structures included in pressure boundary parts are designed complying with KEPIC SNB, concrete structures which are not classified in the boundary parts should conform to KEPIC SNC (KEPIC, 2010a; KEPIC, 2010b; Moon, 2014). In the U.S., design basis and combinations are addressed in the ASME Boiler and Pressure Vessel Code (BPVC) to construct nuclear containment buildings, where loads are divided into service load and factored load categories. Particularly, severe environmental loads, extreme environmental loads, and abnormal loads are involved in the factored load category. Based on the load cases, load combinations and load factors are defined in the ASME code (ACI-ASME Joint Committee, 2015).

A typical research to evaluate the structural capacity about internal pressure was the overpressurization test of a 1:4 scale containment conducted by Sandia National Laboratories. By performing the static pneumatic overpressurization test at ambient temperature, the structural response of the containment to and beyond the design pressure was observed and measured, including the failure modes (Hessheimer, 2003). Akbar and Gupta (1986) studied the reinforced concrete containment behavior under dead load, internal pressure, and earthquake.

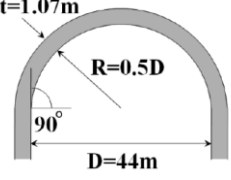
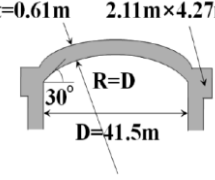
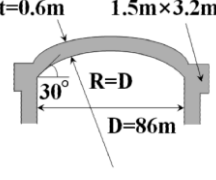
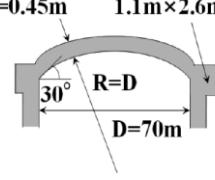
In this study, a containment shell structure subjected to 0.7 MPa of internal pressure is considered. The main purpose of this study is to characterize the behavior when the containment structure is under the extreme internal pressure. Using ETABS 2015 and LS-DYNA, finite element programs, the structural analysis is conducted (CSI, 2015).

## **2. ANALYSIS MODEL**

### *2.1 Computational Model*

Representative types of containment buildings are summarized in Table 1 (Jeon, 2000). In particular, methods of generating nuclear energy are classified as Pressurized Water Reactor (PWR) and Pressurized Heavy Water Reactor (PHWR). The PWR method is employed on the OPR-1000 such as Kori, Hanbit, and Hanul plants. It has a hemispherical dome and cylindrical wall constructed by adopting unbonded prestressed concrete. The PHWR method was applied to the Wolsong plant, where a partially spherical dome was applied on the top of the building. The design pressure was approximately 0.41 MPa and 0.12 MPa, respectively (Kwak, 2004). In Korea, the PWR method was adopted for most of the NPP structures except for 4 units. In this respect, the OPR-1000 is established as a computational model to study a response to internal pressure in this paper.

Table 1 Types of Containment Structures (Jeon, 2000)

Structure	Nuclear Containment Building		LNG Storage Tank	
	OPR-1000 <sup>1)</sup>	CANDU <sup>2)</sup>	Tongyeong	Incheon
Shape of Dome and Ring Beam				
Ring Beam	X	O	O	O

<sup>1)</sup> Optimized Power Reactor 1000 MWe

<sup>2)</sup> Canada Deuterium Uranium

As shown in Fig. 1, a computational containment structure in ETABS 2015 is consisted of cylindrical wall, which has a 22 m radius and 44 m elevation, and a hemispherical dome on the top of the building. The wall and dome thickness is 1.22 m.

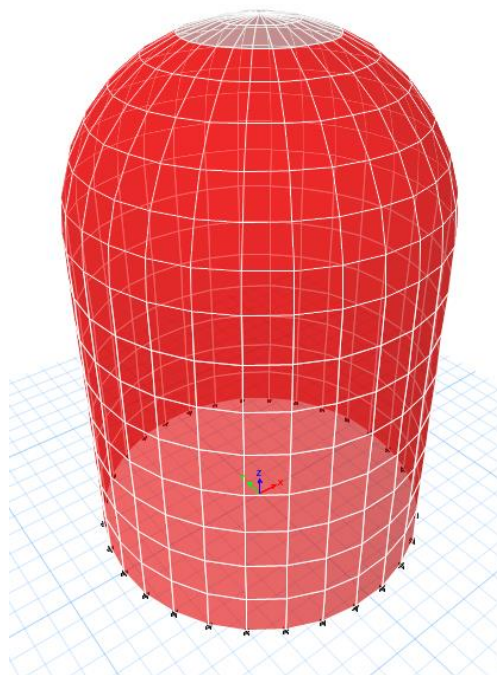


Fig. 1 Computational Shell Structure Model in ETABS 2015

Material properties for concrete are summarized in Table 2 (Lee, 2011). The

compressive strength is 38 MPa, the Poisson's ratio is 0.17, and the density is 0.0025 kg/cm<sup>3</sup>. Equation (1) is used to determine the modulus of elasticity of concrete,  $E_c$ , for normalweight concrete (ACI Committee 318, 2014). Using this equation, the value of the modulus of elasticity is taken as 29,175 MPa.

$$E_c = 57000\sqrt{f'_c} \quad (1)$$

Table 2 Material Properties for Concrete

	Compressive Strength (MPa)	Poisson's Ratio	Density (kg/cm <sup>3</sup> )	Modulus of Elasticity (MPa)
Concrete	38	0.17	0.0025	29175

The value of 0.7 MPa is taken to characterize the structural response under extreme internal pressure. This value is roughly 170% of 0.41 MPa, the design pressure. Therefore, the value of 0.7 MPa is sufficient to evaluate the performance for resisting internal pressure. The pressure is applied to all elements perpendicularly. The self-weight is considered as gravity load.

## 2.2 Assumptions and Restraints

In order to simplify the analysis, the computational model is made up of only wall and dome roof as an axisymmetric structure. Components causing asymmetry such as the equipment hatch and air locking are excluded. Additionally, although the basemat foundation is a flexible bending component for containment structures, it is not established in ETABS 2015. This paper mainly focuses on the elastic behavior of cylindrical wall and dome-shaped roof without consideration of prestressing effects and yielding of the steel.

## 3. RESULTS OF THE ANALYSIS

The elements on a vertical line are selected to examine the data because the computational model maintains the axisymmetric feature. General information about the selected elements is shown in Table 3.

Table 3 General Information of Representative Elements

Height (m)	Shell Object	Unique Name
66.0	F153	213
65.6	F123	183
64.3	W513	153
62.3	W483	123
59.6	W453	93
56.2	W423	60
52.4	W393	33
48.3	W363	3
44.0	W567	409
38.5	W567	410
33.0	W567	411
27.5	W567	412
22.0	W567	413
16.5	W567	414
11.0	W567	415
5.5	W567	416

Figure 2 shows comparisons of the tensile forces or stresses between circumferential and longitudinal directions under design internal pressure. For the tensile force, the maximum force is obtained at 11 m elevation in the circumferential direction. Generally, the circumferential force or stress is larger than that in the longitudinal direction.

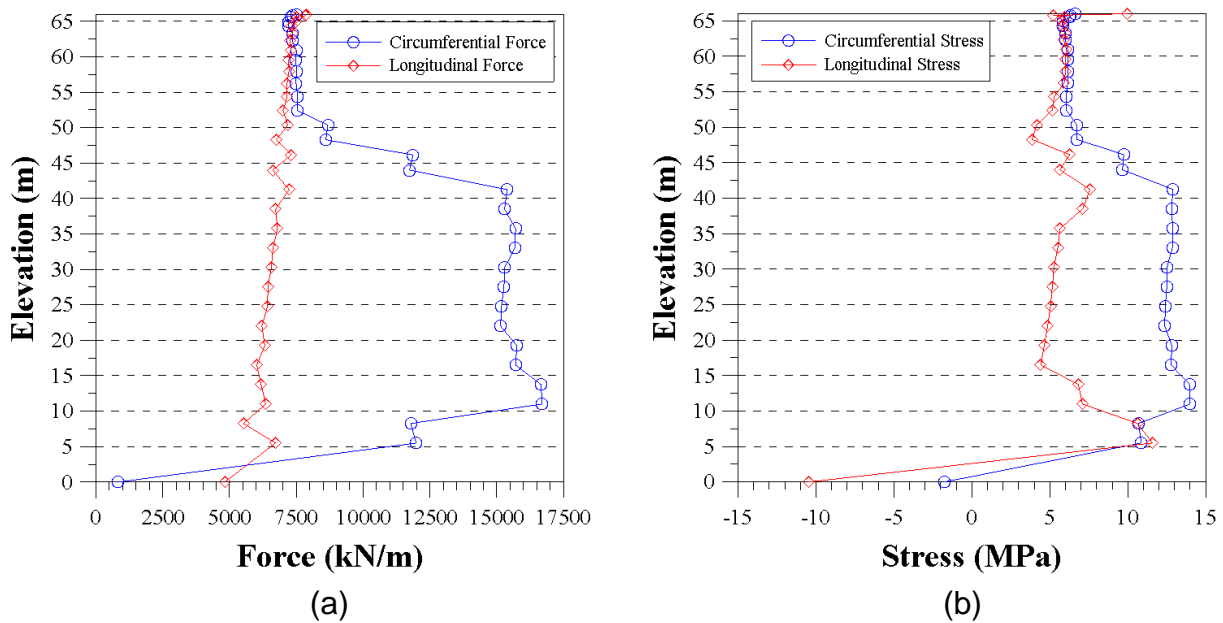


Fig. 2 (a) Tensile Force, (b) Stress

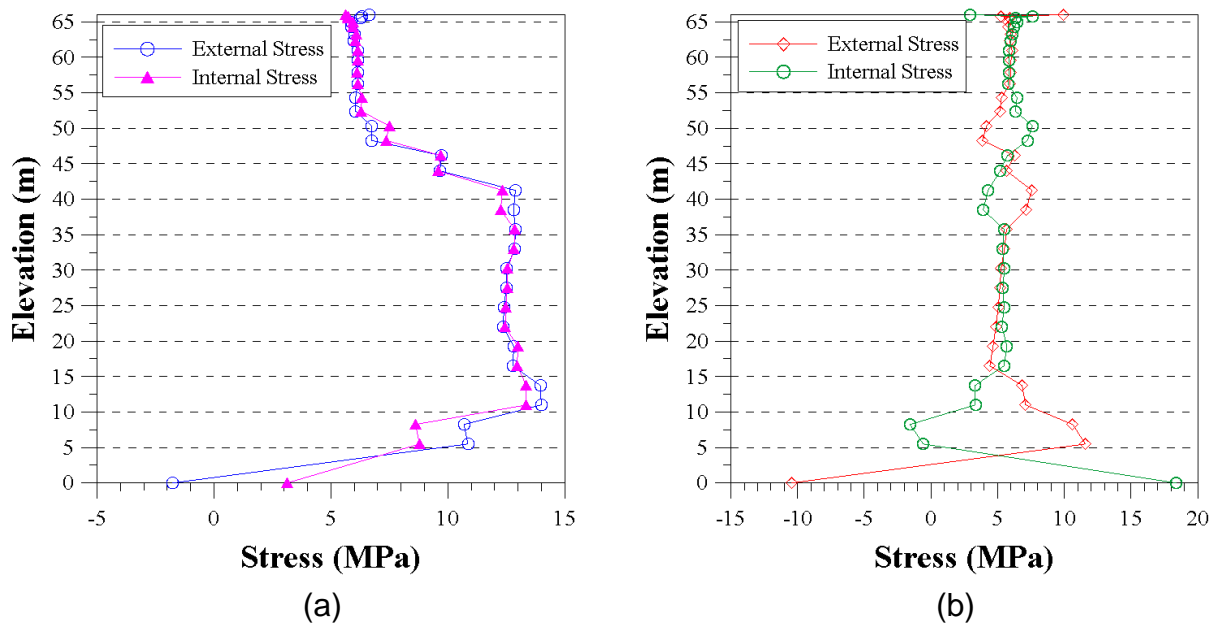


Fig. 3 (a) Circumferential Stress, (b) Longitudinal Stress

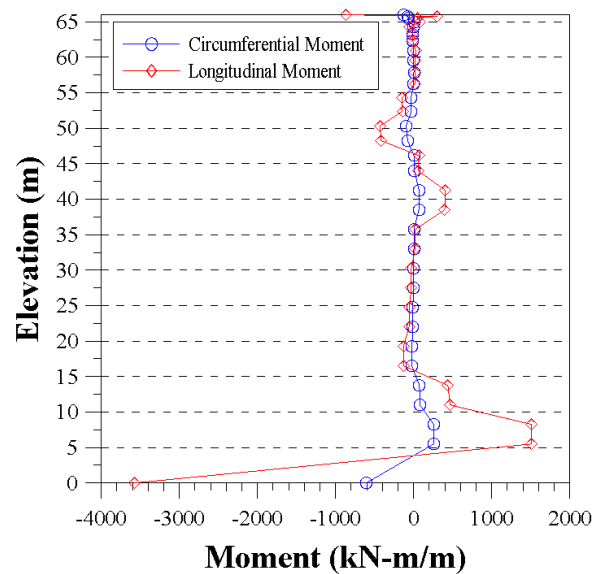


Fig. 4 Moment Comparison

However, as shown in Figs. 3(a) and 3(b), there are differences between the internal and external stress for both directions. A variation in the longitudinal stress is substantial, while a variation in the circumferential direction is quite small. The moments are induced with increasing magnitude of external and internal stress difference. Hence, the pattern of moment is opposite to the tensile force. The moments are observed at the location where stress differences between the external and internal

surfaces are evident as shown in Fig. 4, ranging from 5 m to 11 m in height. Contrary to the circumferential moment which is almost zero, the maximum longitudinal moment is shown at the height of 8 m. The longitudinal moments are close to zero from 11 m to the top of the structure. In conclusion, the stress difference between external and internal wall surfaces is closely related with the moment, and the bending deformation of the containment structure is induced mainly by the longitudinal moment.

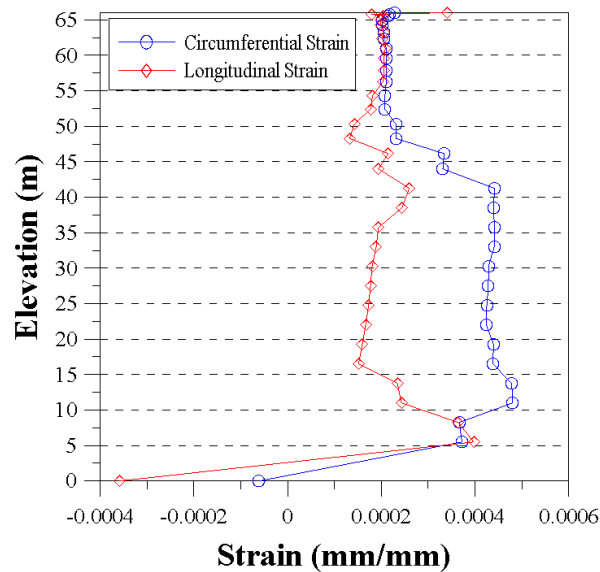


Fig. 5 Strain Comparison

Figure 5 shows the strain of elements for horizontal and longitudinal directions. Both strain values are determined by dividing each stress by the modulus of elasticity of concrete. Therefore the distribution is almost the same shape as that in Fig. 2(b). The maximum circumferential strain of the cylindrical wall is observed at the height of 11 m and shows 0.000439. For longitudinal direction, the maximum strain is 0.000397 at 5.5 m elevation. The strain values are compared with the rupture strain of concrete, where the modulus of rupture for concrete,  $f_r$ , is derived from Eq. (2) of ACI 318-14, and the value of  $\lambda$ , the modification factor, is 1.0 for normalweight concrete. As a result, the value of 3.83 MPa is taken. (ACI 318 Committee, 2014), and the concrete strain at rupture is determined to be 0.00013.

$$f_r = 7.5\lambda\sqrt{f'_c} \quad (2)$$

Circumferential and longitudinal strains exceed the rupture strain of concrete; therefore, it is concluded that crack would occur in all areas of the concrete containment structure without prestressing.

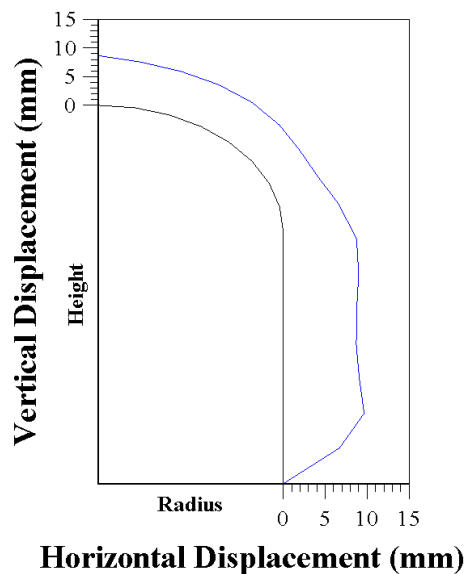


Fig. 6 Deformed Shape of the Containment Structure

The deformed shape of the containment is shown in Fig. 6, which is plotted using displacements in horizontal and vertical directions. Deformation values between the centers of meshes are determined by linear interpolation. A vertical displacement at apex is given by 8.66 mm and a maximum horizontal displacement shows 9.65 mm at 11 m elevation. It is speculated that the horizontal deformation governs the structural behavior of the building under the extreme internal pressure. According to Fig. 2(a) and Fig. 5, maximum values of tensile forces and strains are identified at 11 m elevation. Therefore, it is figured out that the lateral expansion is caused by the circumferential tensile force.

#### 4. LS-DYNA MODELING

Along with the ETABS 2015 analysis, an internal pressure analysis is being conducted, which is in progress using LS-DYNA. This is the finite element method analysis software specialized in and used in large deformation analysis such as the impact, crash, explosion, or collapse. Figure 7 shows the containment structure established in LS-DYNA. Essentially, dimensions of the containment are the same as those used in the ETABS 2015 model. For concrete, \*MAT\_CSCM\_CONCRETE is used and \*MAT\_PLASTIC\_KINEMATIC keyword is employed to establish steel reinforcing bars. The reinforcement modeling embedded in the concrete is executed using \*CONSTRAINED\_LAGRANGE\_IN\_SOLID keyword (LSTC, 2016).

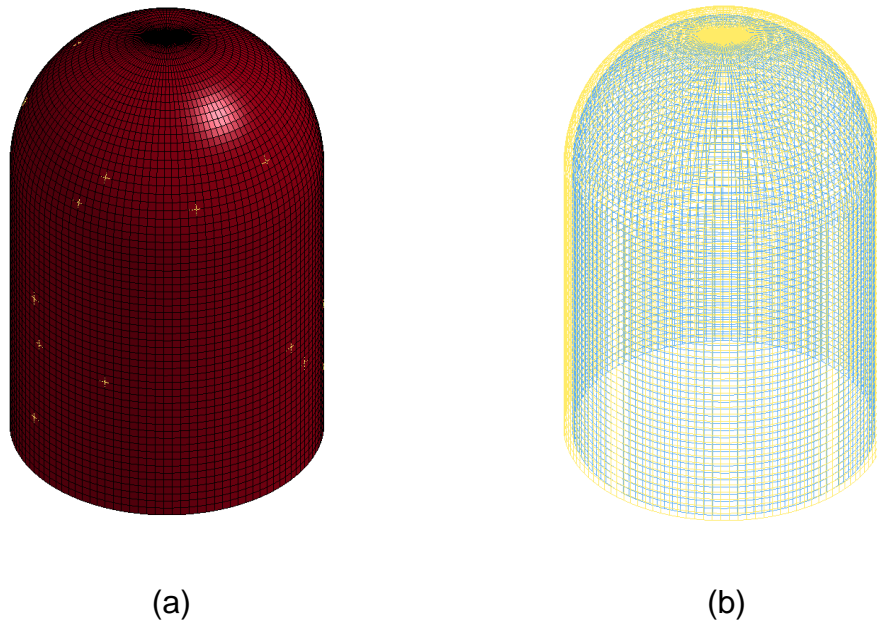


Fig. 7 (a) Overview of the Containment, (b) Reinforcement Modeling

It is confirmed that the displacement induced by gravity load is the same as the result of ETABS 2015 analysis. In the following study, asymmetric factors, such as equipment hatch or entrance, will be considered to improve the accuracy and reliability of results. In addition, it is also planned to conduct a study on comparing structural responses caused by extreme internal pressure.

## 5. CONCLUSION

In the design of containment structures, various load cases and combinations should be considered including implausible cases. Especially, structural safety against extreme internal pressure is important as the containment which plays a role of the radiation shield. In this study, analysis is conducted to characterize the response of the containment subjected to 0.7 MPa pressure. Several conclusions drawn from the analysis are summarized below:

- (1) At 11 m elevation, the maximum tensile force is noted in the circumferential direction.
- (2) Based on the tendency of moments, the maximum moment is obtained at approximately 8 m elevation in the longitudinal direction. Above the height of 11 m, moments in both directions are nearly zero.
- (3) All elements' strain values in both directions are larger than the rupture strain of concrete. Therefore, without prestressing, concrete crack is expected to be observed.
- (4) Overall, the circumferential tensile force and strain are larger than those in the longitudinal direction. In addition, the maximum horizontal displacement is

given by 9.65 mm at 11 m elevation. The structural response of the containment under internal pressure is characterized by the horizontal deformation of the cylindrical wall.

Consequently, the bending behavior is governed by the longitudinal moment, and the tensile force induces expansion. The critical location is where the maximum tensile force and maximum bending moment occur simultaneously. Based on this coupled relationship, the critical location is determined to be at the height of 11 m, although the longitudinal moment is smaller than that below this level.

## ACKNOWLEDGMENT

This research was supported by the National Research Foundation of Korea (NRF) grant (No. 2015-001535). The conclusions in this paper are those of the authors and do not necessarily represent those of the sponsor.

## REFERENCES

- ACI Committee 318 (2014), *Building Code Requirements for Structural Concrete (ACI 318-14) and Commentary (ACI 318R-14)*, American Concrete Institute, Farmington Hills, MI.
- ACI-ASME Joint Committee (2015), *ASME Boiler and Pressure Vessel Code Section III-Division 2 and ACI Standard 359*, The American Society of Mechanical Engineers, New York, NY.
- Akbar, H. and Gupta, A. (1986), "Ultimate Behavior of an R.C. Nuclear Containment Subjected to Internal Pressure and Earthquake", *Journal of Structural Engineering*, Vol. 112(6), 1280-1295.
- CSI (2015), *CSI Analysis Reference Manual*, Computers & Structures, Inc., Berkeley, CA.
- Hessheimer, M. F., Klamerus, E. W., Lambert, L. D., and Rightley, G. S. (2003), *Overpressurization Test of a 1:4-Scale Prestressed Concrete Containment Vessel Model. NUREG/CR-6810, SAND2003-0840P*, Sandia National Laboratories, Albuquerque, NM.
- Jeon, S.-J. and Kim, Y.-J. (2010), "An advanced design procedure for dome and ring beam of concrete containment structures", *Journal of the Korea Concrete Institute*, Vol. 20(6), 817-824. (in Korean)
- KEPIC (2010a), *KEPIC-SNB Concrete Containment*, Korea Electric Association, Songpa, Seoul. (in Korean)
- KEPIC (2010b), *KEPIC-SNC Nuclear Safety-Related Concrete Structures*, Korea Electric Association, Songpa, Seoul. (in Korean)
- Kwak, H.-G., Kim, S.-J., Kim, D.-Y., Kim, S.-H., and Chung, Y.-S. (2004), "Nonlinear analysis of reactor containment structures during ultimate accident condition", *Proceedings of the Korean Nuclear Society Conference*, Gyeongju. (in Korean)
- Lee, H.-P. (2011), "Shell finite element of reinforced concrete for internal pressure analysis of nuclear containment building", *Nuclear Engineering and Design*, Vol.

*The 2016 World Congress on*  
**The 2016 Structures Congress (Structures16)**  
*Jeju Island, Korea, August 28-September 1, 2016*

241(2), 515-525.  
LSTC (2016), *LS-DYNA Keyword User's Manual*, Livermore Software Technology Corporation, Livermore, CA.